Gallium Nitride Nanowire Based Nanogenerators and Light-Emitting Diodes
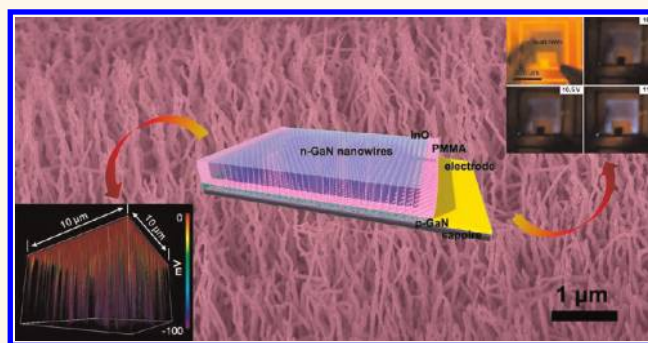
Chih-Yen Chen,[†,‡] Guang Zhu,[†] Youfan Hu,[†] Jeng-Wei Yu,[§] Jinghui Song,[†,⊥] Kai-Yuan Cheng,[‡] Lung-Han Peng,[§] Li-Jen Chou,[‡,*] and Zhong Lin Wang[†,‖,*]

[†]School of Materials Science and Engineering, Georgia Institute of Technology, Atlanta, Georgia, United States, [‡]Department of Materials Science and Engineering, National Tsing-Hua University, Hsinchu, Taiwan, [§]Department of Electrical Engineering and Institute of Photonics and Optoelectronics Engineering, National Taiwan University, Taipei, Taiwan, [⊥]Department of Metallurgical and Materials Engineering, The University of Alabama, Tuscaloosa, Alabama, United States, and [‖]Beijing Institute of Nanoenergy and Nanosystems, Chinese Academy of Sciences, Beijing, China

Energy-harvesting nanotechnology including solar cells,[1,2] fuel cells,[3] thermoelectric generators,[4] and piezoelectric systems[5−7] has attracted intensive interest in the past years. Wurtzite structure materials, such as zinc oxide (ZnO)[5−9] and gallium nitride (GaN),[6,10−12] have been demonstrated as great candidates for piezoelectric nanogenerators and piezotronics. Nanogenerators have successfully demonstrated driving small commercial passive electronic components, such as light-emitted diodes (LEDs), small liquid crystal displays (LCDs), and electronic watches.[13−15] Nanowire-based LEDs are particularly interesting due to the possible advantages of higher lumens, higher efficiency, and lower power consumption than traditional lighting modules. As an important family member of wurtzite structures, GaN nanowires share the same crystal structure as and analogous physical properties with ZnO. In fact, GaN can be the core nanostructures for LED,[16] piezotronics,[6,10−12] and even piezophotonics.[6,17,18] Although the grhowth of GaN nanowires (NWs) have been reported by numerous groups,[19−22] applications of GaN nanowires for nanogenerators and piezotronics are relatively few.

In this paper, a GaN nanowire based nanogenerator and LED are fabricated utilizing n-type GaN nanowires grown on a p-type GaN substrate. The nanogenerator (NG) showed an output power density around ∼12.5 mW/m^2. The images of lighted GaN NWs LEDs and corresponding electroluminescence (EL) spectra have been recorded and investigated. An integrated self-powered LED system totally based on wurtzite-structured materials is demonstrated by using a ZnO piezoelectronic NG

ABSTRACT

Single-crystal n-type GaN nanowires have been grown epitaxially on a Mg-doped p-type GaN substrate. Piezoelectric nanognerators based on GaN nanowires are investigated by conductive AFM, and the results showed an output power density of nearly 12.5 mW/m^2. Luminous LED modules based on n-GaN nanowires/p-GaN substrate have been fabricated. CCD images of the lighted LED and the corresponding electroluminescence spectra are recorded at a forward bias. Moreover, the GaN nanowire LED can be lighted up by the power provided by a ZnO nanowire based nanogenerator, demonstrating a self-powered LED using wurtzite-structured nanomaterials.

KEYWORDS: GaN nanowires · LED · piezoelectric · nanogenerator · self-powered system

combined with energy storage capacitors to light up the LED.

RESULTS AND DISCUSSION

Development of LED Module and Characterization of GaN Nanowires. Figure 1 illustrates a concise fabrication of the final LED modules after providing several procedures for e-beam photolithography, including (i) growing a p-type GaN thin film on a c-plane (0001) sapphire by MOCVD, (ii) depositing a Au catalyst thin film in ultrahigh-vacuum thermal evaporation, (iii) growing n-type
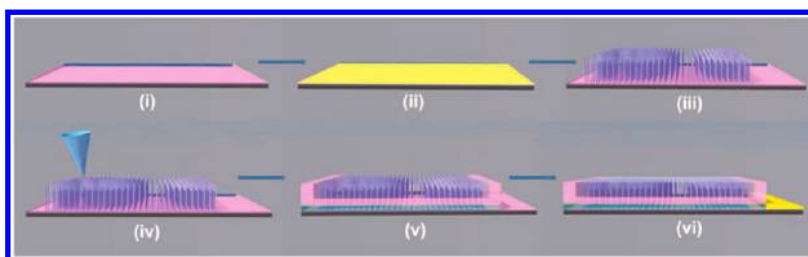
Figure 1. Fabrication flowcharts of a GaN NW LED device, including (i) growth of a p-type GaN thin film on (0001) sapphire, (ii) Au catalyst thin-film evaporation, (iii) growth of n-type GaN NWs, (iv) piezoelectric investigation with an atomic force microscope, (v) spin-coating of a polymer spacer (PMMA) in the LED device, and (vi) deposition of InO and Au/Ni electrodes for n-type and p-type contact, respectively.
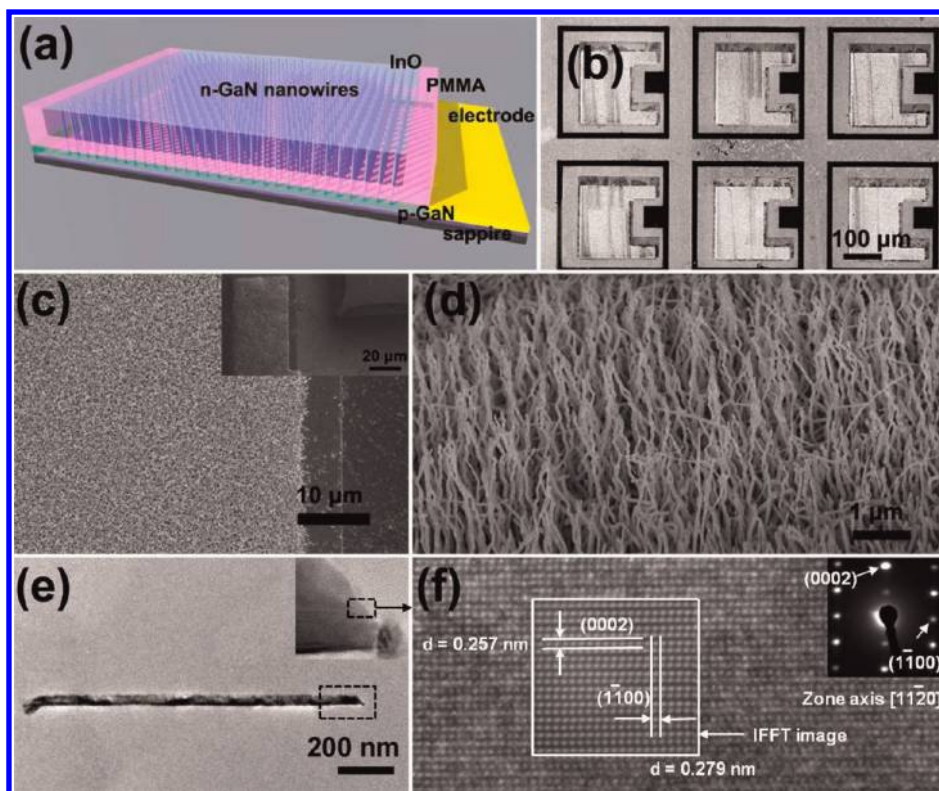

Figure 2. Growth and characterization of GaN NW LEDs on a p-GaN/sapphire (0001) substrate _via_ a V-L-S process. (a) 3D model depicting the detailed structure of the GaN NW LED. (b) Low-magnification SEM image of the LED arrays. (c) Top-view SEM image and its inset showing the high-density GaN NWs grown on the substrate. (d) Tilt-angle SEM image showing the long and free-standing GaN NW grown with a unique orientation. (e) TEM image displaying the diameter of the NW around 50 nm. The inset shows the NW grown _via_ a V-L-S process. (f) HRTEM and selected area diffraction pattern images presenting the growth of the signal-crystal GaN NW with [0001] direction. The inverse fast Fourier transform (IFFT) image indicates a higher resolution crystal structure.

GaN nanowires on a p-type thin film by a vapor—liquid—solid (V-L-S) process, (iv) investigating piezoelectric performance by a unique AFM measurement, (v) spin-coating of polymethyl methacrylate (PMMA) as the binding spacer in LED devices, and (vi) depositing an indium oxide (InO) layer and Au/Ni electrodes for n-type and p-type contact, respectively.

Figure 2a illustrates a briefly three-dimensional structure of the GaN LED devices. The parallel LED arrays are based on n-GaN nanowires/p-GaN substrate structure, and their effective light-emitting area is around 30 000 μm^2, shown in Figure 2b. The SEM images (Figure 2c and d) and the inset show the high density of GaN NWs synthesized on the p-GaN/

sapphire substrate. The free-standing GaN NWs are ~3 μm in length. The diameter of the NWs is ~50 nm, as shown in the TEM image (Figure 2e). A gold nanoparticle catalyst is observed clearly in the high-magnification TEM image (inset of Figure 2e), which suggested that the growth of GaN NWs on the p-GaN substrate was _via_ the V-L-S process.[11,12,22] A high-resolution TEM image and a digitally noise-filtered image are shown in Figure 2f, which depicts our GaN NW grown with single-crystal orientation. In the inset image, the selected area diffraction (SAD) pattern reveals that the GaN NW grows along [0001] due to its perfect match to the p-GaN/sapphire (0001) substrate.
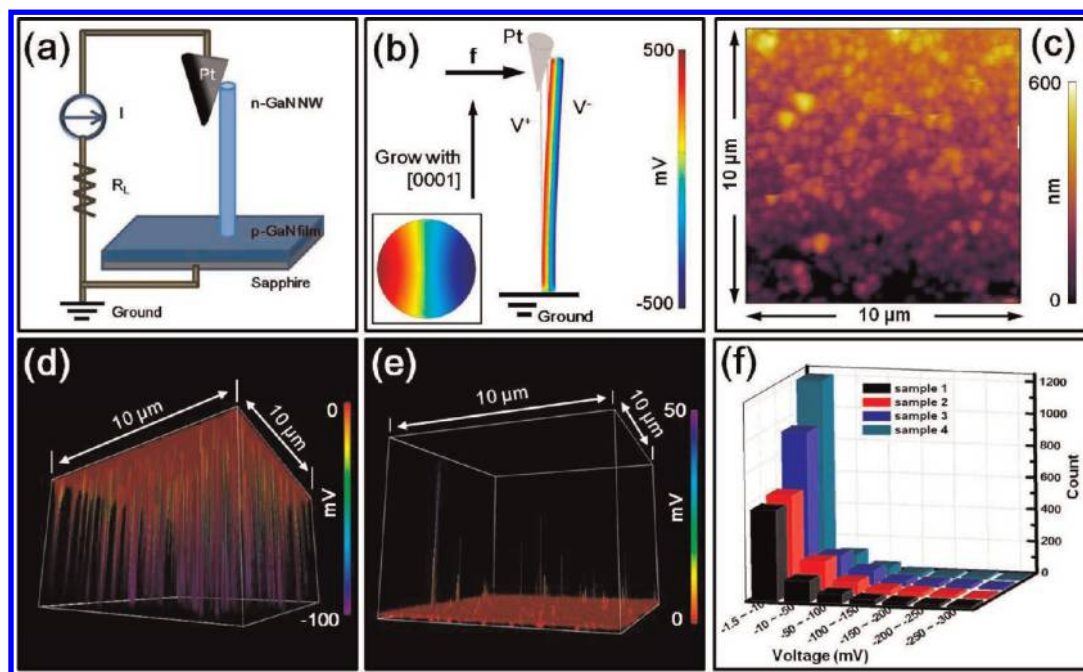
Figure 3. (a) Schematic of AFM measurement setup. (b) Calculated piezopotential distribution at the cross section of a [0001] growth GaN NW with length = 3 μm and diameter = 50 nm. The inset shows a piezopotential distribution in cross section. (c) AFM image revealing the surface of GaN nanowires. (d and e) 3D negative and 3D positive voltage output signals recorded across an external load when scanning over an area of 10 μm $\times$ 10 μm. (f) Statistical distribution of piezoelectric output signal measured from four different GaN NW samples as a function of time to test the stability and reproducibility.

Piezoelectric Nanogenerator of Individual GaN Nanowires. The scheme in Figure 3a presents the experimental setup of using atomic force microscopy (AFM) to characterize the energy-harvesting properties of GaN NWs. The details of the Experimental Methods and the AFM characteristics are similar to our first demonstration of the piezoelectric nanogenerator based on ZnO NWs.[5] The piezoelectric feedback signals of the GaN NWs are characterized utilizing an AFM with the Pt-coated Si tip in contact mode. While the Pt-coated Si tip scans across the GaN NWs, output electrical signals are detected simultaneously from those deformed nanowires, which are continuously recorded across an external load (R_L) of about 500 MΩ. The corresponding simulation result is shown in Figure 3b, which is carried out by using commercial software (COMSOL Multi-physicals 3.5). The color scale distribution reveals the output potential, in which the red and blue areas represent positive and negative output potential, respectively. In addition, the piezopotential distribution depends on the growth direction of the NW. In our case, the GaN NWs were grown along the [0001] orientation. Moreover, the piezopotential distribution in the cross section at the top of the nanowire is shown in the inset of Figure 3b. Some material constants of the GaN NW used in the COMSOL software are given as the following: lattice constants a = 0.319 nm, c = 0.519 nm; transverse isotropy possesses five independent elastic constants, denoted by C_{11} = 390 GP, C_{12} = 145 GP, C_{13} = 106 GP, C_{33} = 398 GP, and C_{44} = 105 GP. The piezoelectric constants are e_{15} = -0.49 C/m^2,

e_{31} = -0.49 C/m^2, and e_{33} = 0.73 C/m^2; relative dielectric constants $\kappa_{11} = \kappa_{12} = \kappa_\perp = 9.28$, $\kappa_{33} = \kappa_\| = 10.01$; and the density $\rho = 6150$ kg/m^3.[10−12] It is assumed that the n-type GaN NWs grow with a [0001] orientation on the p-type GaN substrate. The top side of the nanowire is contacted and pushed by a Pt-coated Si tip with a force of 80 nN. The length and diameter of the GaN nanowire used were 3−4 μm and 50 nm, respectively. The simulation results describe clearly that both the positive and negative signals have a maximum value at the head of the nanowire. The extended surface of the individual GaN NWs demonstrates a positive piezopotential with a magnitude of 500 mV; on the other hand, the compressed part of the GaN NW exhibits a negative magnitude of -500 mV. The topography (feedback signal from the scanner) image of GaN nanowires on the substrate is recorded by AFM in Figure 3c. In contact mode, as the tip scans over the free-standing NWs, the NWs are bent consecutively. The corresponding output voltage signals produced from GaN NWs due to the piezoelectric effect are shown in Figure 3d and e. The data are recorded over the R_L when the AFM tip scans across the GaN nanowire in an area of 100 μm^2, and the color scale stands for the magnitude of the output signal. Figure 3d and e reveal that the GaN NWs generated not only positive output voltage but also a negative one. The real experimental results are consistent with the theoretical trend, which is shown in Figure 3b. Figure 3d and e show that most of the electric outputs belong to the negative signals, and the highest output voltage could
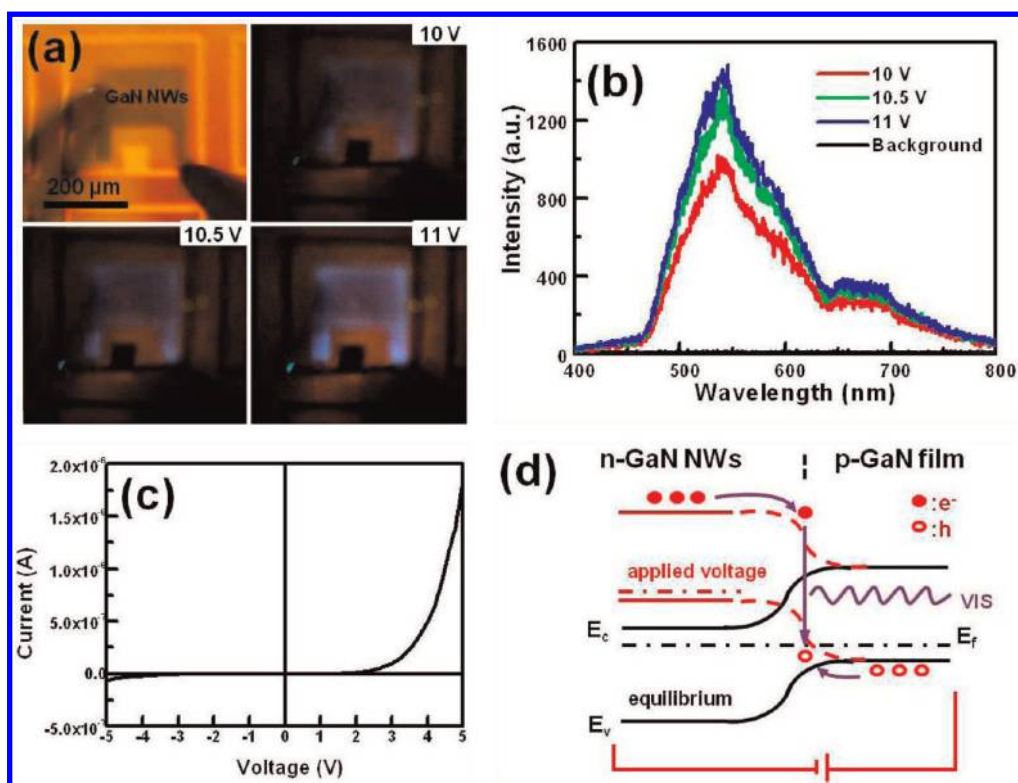
Figure 4. (a) CCD images recorded from a GaN NW LED at forward biases of 10, 10.5, and 11 V, respectively. The representation of the two-terminal device is indicated in the upper-left inset figure. (b) Corresponding electroluminescence spectra of the emitted light at forward biases of 10, 10.5, 11 V. (c) $I-V$ characteristics of GaN NW LED at room temperature, which shows rectifying behavior of a two-terminal device with a threshold voltage of $\sim$2 V. (d) Schematic energy band diagram of the p–n junction under forward bias. The wiggle represents vis (visible light).

reach −300 mV (in Figure 3f). Compared with the negative output signals, only a few of positive output signals could be obtained in Figure 3e. Their positive outputs are relatively lower than the negative ones, and the positive output signals might have a magnitude of 50 mV. For the stability and reliability tests, the piezoelectric outputs of the GaN NWs have been collected from four samples. The statistical data representing the output signal distribution generated by the GaN NWs are shown in Figure 3f. In quantitative analyses, our GaN NWs can generate an average output voltage of about 24.95 mV and average output current of 49.90 pA in an area of 100 μm^2, *i.e.*, a power density around $\sim$12.5 mW/m^2 (see Tables S1 and S2 in the Supporting Information); therefore, we determine that the total maximum self-power output would be around 0.38 mW per GaN NW LED ($\sim$30 000 μm^2).

Figure 4 demonstrates the GaN NW LED's performance. Two microprobes for $I-V$ measurements are positioned on the LED module as shown in the upper left image in Figure 4a. The LED is lighted up with a bright area of 200 μm^2 at voltages of 10, 10.5, and 11 V, respectively. The better luminous efficacy occurs at the forward bias condition during the entire emission process. For LED electroluminescence measurements, its homologous EL spectra shown in Figure 4b have been characterized by a fiberoptics system coupled with the

grating spectrometer (Acton SP-2356 imaging spectro-graph, Princeton Instruments), which covers a visible spectrum range from 400 to 700 nm. The intensity of the EL spectra are increased with increasing injection current at forward bias. Apart from that, two major, broad EL peaks in the visible emission spectra related to point defects and/or impurities are observed, including yellow-band luminescence (540 nm) and orange-band lumines-cence (680 nm). The yellow-band luminescence is a broad emission centered at 2.2–2.3 eV. A number of reports have observed such broad midgap optical transitions in GaN at $\sim$2.2 eV due to the intrinsic defects in n-type or undoped GaN.[16,23,24] The additional data further show the intrinsic band gap state transitions extending from 1.65 to 3.1 eV (400 to 750 nm) below the conduction band edge of the GaN nanowires.[25] The electrical characteristics of p-GaN thin-film/n-GaN NW homojunctions are measured in ambient conditions at room temperature as shown in Figure 4c. The $I-V$ character reveals a rectifying behavior with a threshold voltage of $\sim$2 V. The LED was lighted up under a forward bias, and its energy band diagram is shown in Figure 4d. When the homojunction is forward biased, the electrons emitted from n-GaN NWs recombine continuously with the holes from the p-GaN thin film substrate; therefore, photons with visible (vis) wavelength emit at the p–n junc-tion interface in the LED.[26]
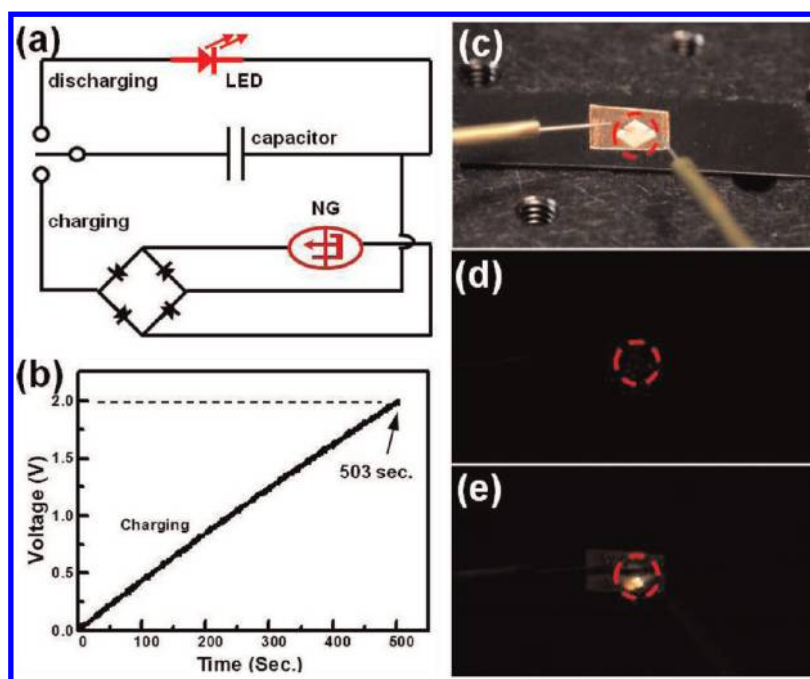
Figure 5. (a) Circuit diagram depicting our self-powered LED system composed of a ZnO NG, rectifying bridges, capacitors, and the GaN LED with a charging and discharging process selecting switch. (b) Charging graph of a supercapacitor, which was fully charged by 10-layer integrated NGs for ~500 s. (c—e) GaN LED was lighted after the capacitors were powered by a 10-layer integrated NG.

Our previous research has shown that NGs based upon ZnO NWs or its hybrid structure can power some electronic devices such as commercial LEDs,[13] electronic watches,[15] and small LCDs.[27] On the other hand, ZnO NGs are also used for highly sensitive environmental sensors for detecting targets such as concentration of Hg^{2+} ion,[13] pH value, or UV photodetector.[7] ZnO NGs with 20 V output voltage have been chosen as the power source for lighting up the GaN LED. Figure 5a shows the designed circuit diagram in which a GaN LED is attached. For the energy-harvesting process, a circuit is connected in the charging loop (Figure 5a) with NGs and a rectifying diode bridge to store generated charge in the capacitor (47 μF, Bennic). After a sufficient charging process, the connection is changed to the discharging loop, when it was ready to light up the GaN NW LED. An energy charging process produced by 10-layer integrated NG[15] has been recorded in Figure 5b. One capacitor is fully charged to 2 V after 503 s by this high-output NG (10 Hz, 1.2 cm vibration distance). Then 10 charged capacitors were connected in series to work as a power supply of approximately 20 V. When the switch is connected with the discharging loop,

the GaN NW LED lights up for 3 s. The lighting processes of the LED are recorded in panels c, d, and e of Figure 5.

CONCLUSION

In conclusion, luminous LED modules based on n-GaN NW arrays, grown epitaxially on the Mg-doped p-GaN substrate, have been fabricated successfully. The statistical distributions of piezoelectric potential produced by GaN nanowires under the deflection of AFM tips were investigated. A maximum output power density was obtained around ~12.5 mW/m^2, *i.e.*, approximately 0.38 mW per GaN NW LED. The better luminous efficacy and their corresponding electroluminescence spectra appear under an increasing forward bias. Moreover, the GaN NWs LED can be driven and lighted up by a self-powered system, which is composed of a 10-layer integrated NG and a charging circuit. On the basis of the above results, the GaN NW LED shows great potential to be utilized for piezoelectric energy generation. A GaN NW LED might be driven by its own internal power output, and it might be able to be operated with low power consumption in future nanotechnology.

EXPERIMENTAL METHODS

n-Type GaN NWs were grown by the V-L-S process. The commercial doped p-type GaN thin film on a *c*-plane (0001) orientated sapphire was chosen as the desired substrate for manufacturing LEDs. The polished *c*-plane sapphire substrate was cleaned with acetone, isopropyl alcohol, and DI water in an

ultrasonic machine. The p-type GaN thin film with (0001) orientation was grown epitaxially on the *c*-sapphire with a thickness of 1.7 μm in a metal organic chemical vapor deposition (MOCVD) system. The concentration of free holes in the film at room temperature reached its maximum value at about 3 × 10^{17}/cm^3 for a magnesium (Mg) doping concentration of about

$10^{18}/cm^3$. After the growth, the p-type GaN on sapphire was loaded immediately into an ultrahigh-vacuum e-gun evaporator for depositing a 5 nm thick Au catalyst layer on the surface. The Ga_2O_3 and graphite powders were used as Ga source and reducing agent, respectively.[28] Ammonia gas (NH_3) was selected as carrier gas and served as the N source for GaN nanowire growth. The mixture of Ga_2O_3 and graphite powders at a weight ratio of 1:5 was put on the alumina boat located in the center of the furnace. Then, the furnace system was heated to 1000 °C at a heating rate of 25 °C/min under a NH_3 flow of 200 sccm. The reaction system was maintained at 1000 °C for 12 h. The morphologies and crystal structures of the as-synthesized nanowires were analyzed with a scanning electron microscope (SEM, LEO-1530). The high-resolution lattice images were obtained with a transmission electron microscope (TEM, JEM-3000F). Finally, the electrical characteristics were measured with contacts deposited with a dual-wire measurement (Keithley, 4200) apparatus. For EL measurements, a fiberoptics system coupled with the grating spectrometer (Acton SP-2356) was chosen for the study.

REFERENCES AND NOTES

1. Tian, B. Z.; Zheng, X. L.; Kempa, T. J.; Fang, Y.; Yu, N. F.; Yu, G. H.; Huang, J. L.; Lieber, C. M. Coaxial Silicon Nanowires as Solar Cells and Nanoelectronic Power Sources. *Nature* **2007**, *449*, 885–890.

2. Law, M.; Greene, L. E.; Johnson, J. C.; Saykally, R.; Yang, P. D. Nanowire Dye-Sensitized Solar Cells. *Nat. Mater.* **2005**, *4*, 455–459.

3. Arico, A. S.; Bruce, P.; Scrosati, B.; Tarascon, J. M.; Van Schalkwijk, W. Nanostructured Materials for Advanced Energy Conversion and Storage Devices. *Nat. Mater.* **2005**, *4*, 366–377.

4. Boukai, A. I.; Bunimovich, Y.; Tahir-Kheli, J.; Yu, J. K.; Goddard, W. A.; Heath, J. R. Silicon Nanowires as Efficient Thermoelectric Materials. *Nature* **2008**, *451*, 168–171.

5. Wang, Z. L.; Song, J. H. Piezoelectric Nanogenerators Based on Zinc Oxide Nanowire Arrays. *Science* **2006**, *312*, 242–246.

6. Wang, Z. L. Progress in Piezotronics and Piezo-Phototronics. *Adv. Mater.* **2012**, 10.1002/adma.201104365.

7. Xu, S.; Qin, Y.; Xu, C.; Wei, Y. G.; Yang, R. S.; Wang, Z. L. Self-powered Nanowire Devices. *Nat. Nanotechnol.* **2010**, *5*, 366–373.

8. Ozgur, U.; Alivov, Y. I.; Liu, C.; Teke, A.; Reshchikov, M. A.; Dogan, S.; Avrutin, V.; Cho, S. J.; Morkoc, H. A Comprehensive Review of ZnO Materials and Devices. *J. Appl. Phys.* **2005**, *98*, 04301.

9. Lee, M.; Chen, C. Y.; Wang, S.; Cha, S. N.; Park, Y. J.; Kim, J. M.; Chou, L. J.; Wang, Z. L. A Hybrid Piezoelectric Structure for Wearable Nanogenerators. *Adv. Mater.* **2012**, *24*, 1759–1764.

10. Bernardini, F.; Fiorentini, V.; Vanderbilt, D. Spontaneous Polarization and Piezoelectric Constants of III−V Nitrides. *Phys. Rev. B* **1997**, *56*, 10024–10027.

11. Huang, C. T.; Song, J. H.; Lee, W. F.; Ding, Y.; Gao, Z. Y.; Hao, Y.; Chen, L. J.; Wang, Z. L. GaN Nanowire Arrays for High-Output Nanogenerators. *J. Am. Chem. Soc.* **2010**, *132*, 4766–4771.

12. Lin, L.; Lai, C. H.; Hu, Y. F.; Zhang, Y.; Wang, X.; Xu, C.; Snyder, R. L.; Chen, L. J.; Wang, Z. L. High Output Nanogenerator Based on Assembly of GaN Nanowires. *Nanotechnology* **2011**, *22*, 475401.

13. Lee, M.; Bae, J.; Lee, J.; Lee, C. S.; Hong, S.; Wang, Z. L. Self-Powered Environmental Sensor System Driven by Nanogenerators. *Energ. Environ. Sci.* **2011**, *4*, 3359–3363.

14. Wang, Z. L. Self-Powered Nanosensors and Nanosystems. *Adv. Mater.* **2012**, *24*, 280–285.

15. Hu, Y. F.; Lin, L.; Zhang, Y.; Wang, Z. L. Replacing a Battery by a Nanogenerator with 20 V Output. *Adv. Mater.* **2012**, *24*, 110–114.

16. Reshchikov, M. A.; Morkoc, H. Luminescence Properties of Defects in GaN. *J. Appl. Phys.* **2005**, *97*, 06301.

17. Wang, Z. L. Piezopotential Gated Nanowire Devices Piezotronics and Piezo-phototronics. *Nano Today* **2010**, *5*, 540–552.

18. Wang, Z. L.; Yang, R. S.; Zhou, J.; Qin, Y.; Xu, C.; Hu, Y. F.; Xu, S. Lateral Nanowire/Nanobelt Based Nanogenerators, Piezotronics and Piezo-phototronics. *Mater. Sci. Eng. R* **2010**, *70*, 320–329.

19. Huang, Y.; Duan, X. F.; Cui, Y.; Lieber, C. M. Gallium Nitride Nanowire Nanodevices. *Nano Lett.* **2002**, *2*, 101–104.

20. Johnson, J. C.; Choi, H. J.; Knutsen, K. P.; Schaller, R. D.; Yang, P. D.; Saykally, R. J. Single Gallium Nitride Nanowire Lasers. *Nat. Mater.* **2002**, *1*, 106–110.

21. Hsieh, C. H.; Chang, M. T.; Chien, Y. J.; Chou, L. J.; Chen, L. J.; Chen, C. D. Coaxial Metal-Oxide-Semiconductor (MOS) Au/Ga$_2$O$_3$/GaN Nanowires: For Nitride Based Logic Nanodevices. *Nano Lett.* **2008**, *8*, 3288–3292.

22. Chen, C. C.; Yeh, C. C.; Chen, C. H.; Yu, M. Y.; Liu, H. L.; Wu, J. J.; Chen, K. H.; Chen, L. C.; Peng, J. Y.; Chen, Y. F. Catalytic Growth and Characterization of Gallium Nitride Nanowires. *J. Am. Chem. Soc.* **2001**, *123*, 2791–2798.

23. Li, G.; Chua, S. J.; Xu, S. J.; Wang, W.; Li, P.; Beaumont, B.; Gibart, P. Nature and Elimination of Yellow-Band Luminescence and Donor Acceptor Emission of Undoped GaN. *Appl. Phys. Lett.* **1999**, *74*, 2821–2823.

24. Hofmann, D. M.; Kovalev, D.; Steude, G.; Meyer, B. K.; Hoffmann, A.; Eckey, L.; Heitz, R.; Detchprom, T.; Amano, H.; Akasaki, I. Properties of the Yellow Luminescence in Undoped GaN Epitaxial Layers. *Phys. Rev. B* **1995**, *52*, 16702–16706.

25. Carter, D. J.; Gale, J. D.; Delley, B.; Stampfl, C. Geometry and Diameter Dependence of the Electronic and Physical Properties of Gallium Nitride Nanowires from First Principles. *Phys. Rev. B* **2008**, *77*, 12. 115339.

26. Yeh, P. C.; Hwa, M. C.; Yu, J. W.; Wu, H. M.; Tsai, H. L.; Lai, C. M.; Huang, J. J.; Yang, J. R.; Peng, L. H. Photon-aAssisted Tunneling in GaN Nanowire White Light Emitting Diodes. *Phys. Status Solidi C* **2009**, *6*, 538–540.

27. Hu, Y. F.; Zhang, Y.; Xu, C.; Zhu, G. A.; Wang, Z. L. High-Output Nanogenerator by Rational Unipolar Assembly of Conical Nanowires and Its Application for Driving a Small Liquid Crystal Display. *Nano Lett.* **2010**, *10*, 5025–5031.

28. Chen, P. H.; Hsieh, C. H.; Chen, S. Y.; Wu, C. H.; Wu, Y. J.; Chou, L. J.; Chen, L. J. Direct Observation of Au/Ga$_2$O$_3$ Peapodded Nanowires and Their Plasmonic Behaviors. *Nano Lett.* **2010**, *10*, 3267–3271.